

Monte Carlo investigation of terahertz plasma oscillations in gated ultrathin channel of *n*-InGaAs

J.-F. Millithaler,^{1,a)} J. Pousset,¹ L. Reggiani,¹ P. Ziade,² H. Marinchio,² L. Varani,² C. Palermo,² J. Mateos,³ T. González,³ S. Perez,³ and D. Pardo³

¹Dipartimento di Ingegneria dell'Innovazione and CNISM, Università del Salento, 73100 Lecce, Italy

²Institut d'Electronique du Sud, UMR CNRS 5214, Université Montpellier II, Place Bataillon, 34095 Montpellier Cedex 5, France

³Departamento de Física Aplicada, Universidad de Salamanca, Pza. Merced s/n, 37008 Salamanca, Spain

(Received 18 August 2009; accepted 23 September 2009; published online 12 October 2009)

By numerical simulations we investigate the dispersion of the plasma frequency in a gated channel of *n*-type InGaAs layer of thickness *W* and submicron length *L* at *T*=300 K. In the presence of a source-drain voltage and for a carrier concentrations of 10^{18} cm⁻³ the spectra evidences a peaked shape with two main bumps, the former at high frequency corresponding to the three-dimensional plasma frequency and the latter at a low frequency. The frequency value of the latter peak exhibits a dispersion as the inverse of the channel length in agreement with the predictions of gradual channel approximation. At increasing drain voltages the instabilities associated with the presence of Gunn domains are responsible for a suppression of the plasma peak in favor of the onset of a peak in the subterahertz domain associated with transit time effects. © 2009 American Institute of Physics. [doi:10.1063/1.3248096]

Generation and detection of electromagnetic radiation in the terahertz domain is a subject in fast development because of its potential applications in different branches of advanced technologies, such as broadband communications, high-resolution spectroscopy, medical, and biological imaging, security, etc.^{1,2} As a consequence, the realization of solid-state devices operating in the terahertz domain at room temperature and with compact, powerful, and tunable characteristics is a mandatory issue. To this purpose, one of the most promising strategies lies in the plasmonic approach, which exploits the plasma frequency associated with long range Coulomb interaction of charge carriers as a possible mechanism for terahertz detection/generation.³

In bulk semiconductors, the plasma frequency is given by the simple expression

$$f_p^{3D} = \frac{1}{2\pi} \sqrt{\frac{e^2 n_0^{3D}}{m_0 m \epsilon_0 \epsilon_{\text{mat}}}}, \quad (1)$$

with *e* the absolute value of the electron charge, n_0^{3D} the three-dimensional (3D) average carrier concentration, m_0 and *m* the free and effective electron masses, respectively, and ϵ_0 , ϵ_{mat} the vacuum permittivity and the relative dielectric constant of the bulk material, respectively. For carrier concentrations of about 10^{17} cm⁻³ the plasma frequency is in the terahertz range for most materials.

For the case of a gated channel, within the gradual channel approximation (GCA) the two-dimensional (2D) electron gas was found to behave as the support of 2D plasma waves with fundamental frequency⁴

$$f_p^{2D \text{ gated}} = \frac{1}{2\pi} \sqrt{\frac{e^2 n_0^{2D} d k^2}{m_0 m \epsilon_0 \epsilon_{\text{diel}}}}, \quad (2)$$

where *d* is the gate to channel distance, $n_0^{2D} = n_0^{3D} \cdot W$ is the average 2D carrier concentration, ϵ_{diel} the relative dielectric

constant of the external dielectric, and *k* the plasma wave vector. Expression (2) was obtained for boundary conditions corresponding to a constant value of the potential at the source and a constant value of the current at the drain contact, respectively. We notice that a practical realization of these boundary conditions within a Monte Carlo simulator remains an open problem. The 2D plasma frequency is dispersive, i.e., $f_p^{2D} = f_p^{2D}(k)$ and depends on the relative dielectric constant of the external dielectric. Through these plasma oscillations, nanometric high electron mobility transistors provided experimental evidence as emitter and/or detector of electromagnetic radiation in the terahertz range.⁵

This work investigates a gated channel semiconductor structure from a microscopic point of view, thus testing the predictions of the simplified analytical approaches and providing more physical insight into the problem. To this purpose, we consider an *n*-type In_{0.53}Ga_{0.47}As layer within a gated configuration at room temperature, and investigate the plasma frequency characteristics by analyzing the frequency spectrum of voltage fluctuations extracted from inside (preferably in the center) the channel obtained from a Monte Carlo simulator coupled with a 2D Poisson solver. As boundary conditions we follow previous works on the subject^{6,7} and use an Ohmic contact at the source (zero constant voltage) and a constant applied voltage at the drain. The time and space discretizations take typical values of 0.2–10 fs for the time step, 0.1–2 nm for the spatial scale of the bar, 500 nm for the spatial scale of the dielectric. Contacts are permeable to carrier crossing in both longitudinal directions, while in the transverse direction at the interfaces carriers are reflected inside the channel. Accordingly, the random motion of free carriers is responsible of voltage fluctuations inside the channel and the presence of a dielectric discontinuity at the interface of a modulation of the plasma frequency with respect to its 3D value. The analogous case of an ungated structure was already considered in a previous publication^{6,7} and it can be a valuable source of comparison with present

^{a)}Electronic mail: jf.millithaler@unile.it.

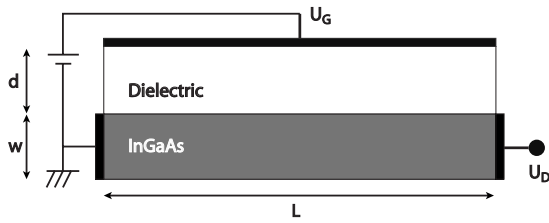


FIG. 1. Schematic of the gated structure with the three terminals.

findings. In the GCA, the plasma frequency f_p can be also conveniently expressed as

$$f_p = \sqrt{\frac{eU}{m_0 m}} \times \frac{k}{2\pi}, \quad (3)$$

with $U = U_G - U_C - U_T$, where U_T is the threshold voltage, $(U_G - U_C)$ is the gate to channel voltage, and $U = en_0^{2D}/C$ with $C = \epsilon_0 \epsilon_{\text{diel}}/d$ the gate to channel capacitance per unit surface.

Figure 1 shows a sketch of the structure under simulation. As typical values of the parameters, if not stated otherwise, we take the following: the gate to channel length $d = 20$ nm, the channel thickness $W = 10$ nm, the drain potential $U_D = 0.01$ V, the gate to source potential $U_G = 1$ V, and the channel length L and the carrier concentration as variables.

In the absence of a net current ($U_D = 0$ V) the simulations evidence the only presence of the plasma peak in the spectrum of voltage fluctuations at a frequency corresponding to that of the 3D case (10 THz). By changing the values of (i) the gate voltage (from 0.1 to 5 V), (ii) the channel length (from 0.1 to 1 μm), and (iii) the channel thickness (from 1 to 10 nm), the frequency value of the 3D plasma peak does not change significantly.

In the following we exploit the influence of the presence of a net current in the channel. We first consider a value of the drain voltage sufficiently small to be in the Ohmic region of response, and then consider the case of a drain voltage sufficiently high for the onset of current saturation and/or negative differential conductivity conditions.

Figure 2 reports the spectral density of voltage fluctuations extracted in the middle of the channel for $n_{3D} = 10^{18} \text{ cm}^{-3}$ and different lengths. The spectra exhibit a structure with a first peak centered at about 10 THz and a second one shifting at lower frequencies at increasing length following a $1/L$ behavior, as predicted by the GCA, within an accuracy of a factor 2 at worst. We notice that the high peak value of 10 THz corresponds to the 3D value at the given concentration. In the absence of a dielectric discontinuity at the channel insulator interface, i.e., by taking $\epsilon_{\text{diel}} = 13.88$, the spectra do not evidence the presence of sharp peaks but rather a broad structure well below the value of the low frequency plateau, before cutoff at the highest frequencies. Furthermore, at increasing channel lengths the presence of resonant frequencies at values above the fundamental 2D peak is evidenced. These oscillations are related to the resonant excitation of spatial modes of plasma waves in the dielectric layer separating the channel from the gate.⁸

Figure 3 reports the peaks of the 2D plasma frequency in the middle of the channel exhibited by simulations as a function of the channel length at two carrier concentrations. Symbols refer to simulations and lines to the theoretical predictions of Eq. (2) with the choice $k = \pi/(\sqrt{2}L)$, with L the

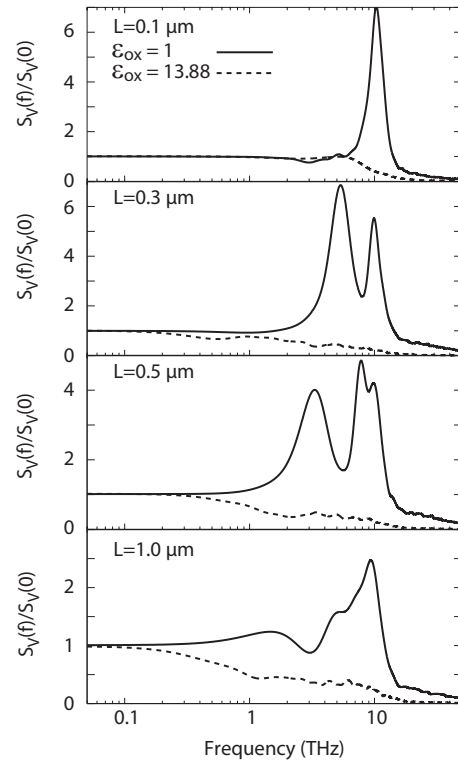


FIG. 2. Normalized spectral density of voltage fluctuations for different channel lengths and carrier concentration 10^{18} cm^{-3} , $W = 10$ nm, and $U_D = 0.01$ V. Continuous (dashed) curves refer to the presence (absence) of a dielectric discontinuity at the interface between the channel and the insulator under the gate.

channel length. The inset in Fig. 3 reports the expected scaling of f^{2D} with the dielectric thickness. The agreement found is within the numerical uncertainty, estimated to be at worst within 20%, and validates the main predictions of the analytical theory. We notice that the spectra taken for different values of the thickness W in the range of 1–20 nm are quite similar to each other and the case $W = 10$ nm is found to better reproduce the theoretical expectation.

Figure 4 compares the noise spectra of voltage fluctuations in the presence of an increasing of the applied voltage up to values sufficiently high (1 V) for the onset of Gunn instabilities.⁹ The results show that the presence of the Gunn instabilities suppresses totally the plasma peak of the voltage spectral density and is responsible of a sharp peak at the Gunn domain transit time frequency of about 0.1 THz. When

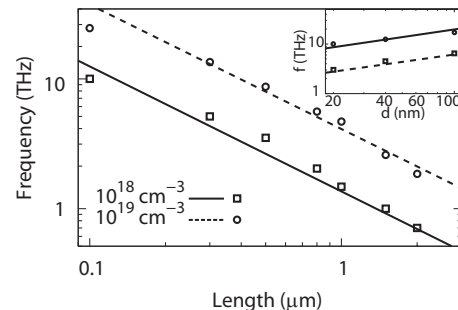


FIG. 3. Frequency of the second peak attributed to the 2D plasma peak as a function of the length of the channel for carrier concentrations of 10^{18} and 10^{19} cm^{-3} . The inset reports the same quantity as function of the dielectric thickness. Symbols refer to simulations and lines to theoretical predictions of Eq. (2).

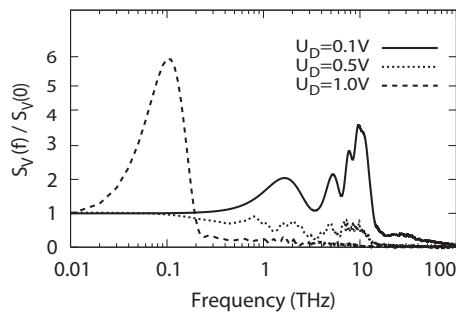


FIG. 4. Transition from plasma to Gunn of the voltage spectrum peak at increasing values of the drain voltage for a carrier concentration 10^{18} cm^{-3} , $L=1 \text{ }\mu\text{m}$, $W=10 \text{ nm}$, and $U_G=1 \text{ V}$.

comparing the emergence of Gunn effect here with that of the ungated structure,⁷ we find that for the same set of parameters the presence of the gate is responsible of a significant suppression (up to about a factor of 50) of the height of the plasma peak which is also broadened. Accordingly, the possibility of current oscillations is limited by the presence of the gate, as expected. Another advantage of the gated structure is a greater sensitivity of the plasma peak to the channel length (scaling as $1/L$) with respect to the ungated structure (scaling as $1/\sqrt{L}$). Furthermore, the 2D carrier concentration (and thus the plasma frequency) can be modulated directly by the gate bias.

In conclusions, within a microscopic Monte Carlo simulator we have investigated the plasmonic peaks associated with voltage fluctuations spectra in *n*-type InGaAs gated structure of nanometric sizes. The main results of the present investigation are summarized as follows. In the presence of a net current in the channel we observed the onset of a plasma peak at frequency below that of a 3D electron gas, whose dispersion follows that of a 2D electron gas predicted within the gradual channel approximation. The presence of a dielectric discontinuity at the interface between the channel and the

dielectric is found to substantially amplify the plasma peaks. Harmonics above the fundamental 2D frequency are detected at increasing channel lengths. The presence of a high source-drain voltage able to establish Gunn domains washes out all the plasma peaks in favor of the onset of a Gunn peak at a lower frequency within the 0.1 THz range which is related to transit time effects.

The work was supported by LAVOISIER GRANT (J. Pousset), CNRS-GDR and GDR-E projects “Semiconductor sources and detectors of THz frequencies,” Region Languedoc-Roussillon—project “Plateforme Technologique THz,” the Dirección General de Investigación (MEC, Spain), FEDER through Project No. TEC2007-61259/MIC, Accion Integrada Project No. HF2007-0014, and by the Consejería de Educación of the Junta de Castilla y León (Spain) through Project Nos. SA019A08 and GR270.

¹D. L. Woolard, E. R. Brown, M. Pepper, and M. Kemp, *Proc. IEEE* **93**, 1722 (2005).

²V. Ryzhii, *J. Phys.: Condens. Matter* **20**, 380301 (2008).

³A. El Fatimy, R. Tauk, S. Boubanga, F. Teppe, N. Dyakonova, W. Knap, J. Lyonnet, Y. M. Meziani, T. Otsuji, M.-A. Poisson, E. Morvan, S. Bollaert, A. Shchepetov, Y. Roelens, Ch. Gaquiere, D. Theron, and A. Cappy, *Phys. Status Solidi C* **5**, 244 (2008).

⁴M. Dyakonov and M. S. Shur, *Phys. Rev. Lett.* **71**, 2465 (1993).

⁵J. Lusakowski, W. Knap, N. Dyakonova, L. Varani, J. Mateos, T. González, Y. Roelens, S. Bollaert, A. Cappy, and K. Karpierz, *J. Appl. Phys.* **97**, 064307 (2005).

⁶J.-F. Millithaler, L. Reggiani, J. Pousset, L. Varani, C. Palermo, W. Knap, J. Mateos, T. González, S. Perez, and D. Pardo, *Appl. Phys. Lett.* **92**, 042113 (2008).

⁷J.-F. Millithaler, L. Reggiani, J. Pousset, G. Sabatini, L. Varani, C. Palermo, J. Mateos, T. González, S. Perez, and D. Pardo, *J. Phys.: Condens. Matter* **20**, 384210 (2008).

⁸P. Shiktorov, E. Starikov, V. Gruzinskis, L. Varani, G. Sabatini, H. Marinchio, and L. Reggiani, *J. Stat. Mech.: Theory Exp.* **B09**, 1742 (2009).

⁹H. Kroemer, *Proc. IEEE* **52**, 1736 (1964).